Journal of Physics A: Mathematical and Theoretical

PAPER • OPEN ACCESS

Stationary state degeneracy of open quantum systems with non-abelian symmetries

OPEN ACCESS
IOP Publishing
Journal of Physics A: Mathematical and Theoretical
J. Phys. A: Math. Theor. **53** (2020) 215304 (17pp)
https://doi.org/10.1088/1751-8121/ab88e3

Stationary state degeneracy of open quantum systems with non-abelian symmetries

Zh Zhang[1,2], J Tindall[1], J Mur-Petit[1], D Jaksch[1] and B Buča[1,3]

[1] Clarendon Laboratory, University of Oxford, Parks Road, Oxford OX1 3PU, United Kingdom
[2] Department of Physics, Tsinghua University, Beijing 100084, People's Republic of China

E-mail: berislav.buca@physics.ox.ac.uk

Received 30 December 2019, revised 19 March 2020
Accepted for publication 14 April 2020
Published 4 May 2020

CrossMark

Abstract
We study the null space degeneracy of open quantum systems with multiple non-abelian, strong symmetries. By decomposing the Hilbert space representation of these symmetries into an irreducible representation involving the direct sum of multiple, commuting, invariant subspaces we derive a tight lower bound for the stationary state degeneracy. We apply these results within the context of open quantum many-body systems, presenting three illustrative examples: a fully-connected quantum network, the XXX Heisenberg model and the Hubbard model. We find that the derived bound, which scales at least cubically in the system size the SU(2) symmetric cases, is often saturated. Moreover, our work provides a theory for the systematic block-decomposition of a Liouvillian with non-abelian symmetries, reducing the computational difficulty involved in diagonalising these objects and exposing a natural, physical structure to the steady states—which we observe in our examples.

Keywords: Lindblad master equation, symmetry, degeneracy, non-ergodicity, open quantum systems, quantum Liouvillians, quantum networks

(Some figures may appear in colour only in the online journal)

[3] Author to whom any correspondence should be addressed.

1. Introduction

Understanding ergodicity in quantum many-body systems remains a fundamental task of mathematical physics. The notion of symmetries plays a crucial role in determining the dynamics and long-time behaviour [1–7]. For closed many-body systems the existence of extensive symmetries (e.g. due to the underlying integrability, or localization of the model) can lead to the absence of both thermalization and ergodicity [8–15].

Understanding non-ergodicity of open quantum systems is seemingly more difficult. For finite-size systems within the Markovian approximation, i.e. when the time dynamics can be described in the Lindblad master equation framework [16–18], the question is partially resolved [19–22]. It is known that specific kinds of symmetries called *strong symmetries* [20] lead to degeneracy of the (time-independent) stationary state to which the open system evolves in the long-time limit. This result connecting the structure of the symmetry operator and the degeneracy of the stationary state has allowed research into many interesting questions, e.g. quantum memory storage and manipulation [23], quantum metrology [24], quantum batteries [25], quantum transport [26, 27], exact solutions [28], potential probes of molecular structure [29], dissipative state preparation [30, 31], correlation functions [32] and thermalization and relaxation [33–35]. Furthermore, degeneracy of the stationary states can be a starting point for realizing discrete time crystals under dissipation [36–38].

The strong symmetry theorem [20] has thus far been limited to abelian symmetries, i.e. symmetries whose corresponding operators all commute with each other. In this article we derive a lower bound for the stationary-state degeneracy of an open quantum system with multiple, non-abelian strong symmetries—symmetries whose corresponding operators do not necessarily commute. We achieve this through decomposing the matrix representation of these symmetries into a series of irreducible representations[4]. As illustrative examples, we apply our theory to three archetypal models: a quantum network, the open randomly dissipative XXX Heisenberg model and the spin-dephased Fermi–Hubbard model. The models are interesting for understanding transport in molecules and quantum networks [26, 39], the effects of disorder on relaxation, and out-of-equilibrium superconductivity [40]. We also study the XXX model under collective dissipation as a simple toy example. Using our theory we are able to derive a tight bound for the stationary state degeneracy in each case, finding that, numerically, this bound is saturated in most situations.

The stationary-state degeneracy in the XXX spin chain and Hubbard model examples, which scales at least cubically in the system size, provides a space for the storage of quantum information—despite the presence of environmental noise. Moreover, our work provides a theory for the systematic block-decomposition of a Liouvillian with non-abelian symmetries, reducing the computational difficulty involved in diagonalising these objects and exposing a natural, physical structure to the steady states which we observe in our examples.

2. Theoretical lower bounds on the stationary state degeneracy of an open quantum system

Under the Markov approximation [16–18, 41], the dynamical evolution of an open quantum system can be described by the Lindblad master equation (here, and in the remainder of this work, we set $\hbar = 1$)

[4] In this case the irreducible representations correspond to matrices which cannot be further block diagonalised.

$$\dot{\rho} = \mathcal{L}\rho = -\mathrm{i}[H, \rho] + \sum_l \gamma_l (2L_l \rho L_l^\dagger - \{L_l^\dagger L_l, \rho\}), \tag{1}$$

where ρ is the density matrix of the system, $\mathcal{L}$ is the Liouvillian superoperator acting on the space of bounded linear operators $\mathcal{B}(\mathcal{H})$. The Hamitonian H in equation (1) describes the coherent evolution of the system, while the Lindblad 'jump' operators L_l describe the interactions between the system and the environment with corresponding coupling strengths γ_l.

We also define the adjoint of the master equation via the standard Heisenberg picture for the observable O: $\langle O(t)\rangle = \mathrm{tr}\left(O\ \exp(\hat{\mathcal{L}}t)\rho(0)\right) = \mathrm{tr}\left(\exp(\hat{\mathcal{L}}^\dagger t) O \rho(0)\right)$ (expanding the exponential),

$$\dot{O} = \hat{\mathcal{L}}^\dagger O = \mathrm{i}[H, \rho] + \sum_l \gamma_l (2L_l^\dagger \rho L_l - \{L_l^\dagger L_l, \rho\}), \tag{2}$$

which also defines the adjoint Liouvillian superator $\hat{\mathcal{L}}^\dagger$.

2.1. Stationary state degeneracy in the presence of an abelian strong symmetries

As a starting point for our theory we describe the nullspace degeneracy of an open quantum system in the presence of a single strong symmetry [20]. A strong symmetry S of the Lindblad equation is a symmetry whose operator representation $R(S)$ satisfies the commutation relations

$$[H, R(S)] = 0, \quad [L_l, R(S)] = [L_l^\dagger, R(S)] = 0, \quad \forall l. \tag{3}$$

Now suppose $R(S)$ has n_s different eigenvalues. Then we can decompose the Hilbert space into the corresponding blocks for each eigenvalue

$$\mathcal{H} = \bigoplus_{\alpha=1}^{n_\mathrm{s}} \mathcal{H}_\alpha, \tag{4}$$

with α indexing the different blocks. Moreover, we can carry this decomposition through to the space of bounded linear operators $\mathcal{B}(\mathcal{H}) = (\mathcal{H}, \mathcal{H})$

$$(\mathcal{H}, \mathcal{H}) = \bigoplus_{\alpha=1}^{n_\mathrm{s}} \bigoplus_{\alpha'=1}^{n_\mathrm{s}} (\mathcal{H}_\alpha, \mathcal{H}'_\alpha), \tag{5}$$

where the Liouvillian is block-diagonal, i.e. $\mathcal{L}$ cannot move states between any of the the n_s^2 subspaces which are indexed by α and α'

$$\mathcal{L}(\mathcal{H}_\alpha, \mathcal{H}'_\alpha) \subseteq (\mathcal{H}_\alpha, \mathcal{H}'_\alpha); \tag{6}$$

this follows from (3). Furthermore, it can be proven, due to trace preservation of the dynamics, that in every diagonal subspace $(\mathcal{H}_\alpha, \mathcal{H}_\alpha)$ there is at least 1 stationary state of $\mathcal{L}$ [20]. Hence, the stationary-state degeneracy of a system with a single strong symmetry has a lower bound of n_s.

2.2. Stationary state degeneracy in the presence of multiple abelian strong symmetries

We now move on to the case where there are multiple, abelian symmetries, i.e. there exists a series of symmetries $\{S_1, S_2, \ldots, S_n\}$ whose operator representations $R(S_k)$ in $\mathcal{B}(\mathcal{H})$, which are all linearly independent, satisfy

$$[H, R(S_k)] = 0, \quad [L_l, R(S_k)] = [L_l^\dagger, R(S_k)] = 0 \quad [R(S_k), R(S_{k'})] = 0, \quad \forall l, k, k'. \tag{7}$$

Now suppose $R(S_1)$ has n_1 distinct eigenvalues; then we can decompose the Hilbert space into a series of blocks specified by these eigenvalues for this first strong symmetry

$$\mathcal{H} = \bigoplus_{\alpha=1}^{n_1} \mathcal{H}_\alpha. \tag{8}$$

We now repeat this procedure, decomposing each H_α into $n_{\alpha,2}$ blocks which label the distinct eigenvalues of $R(S_2)$ within the α block. We continue this blocking procedure until we have completely decomposed the space into a series of N spaces. Following our block-decomposition, we then use an identical argument to the previous section and carry this through to $\mathcal{B}(\mathcal{H})$, noting the Liouvillian has at least 1 unique steady state in the diagonal spaces.

As a result, the stationary state degeneracy is lower bounded by N, which is the number of permitted distinct combinations of the eigenvalues of the matrices $\{R(S_1), R(S_2), \ldots, R(S_n)\}$ (for example there might be eigenvalues of $R(S_k)$ for which certain eigenvalues of $R(S_{k'})$ are not possible). We note that the minimum value of N is therefore $\max(\{n_k\})$ and its maximum is $\prod_{k=1}^{n} n_k$ where n_k is the number of distinct eigenvalues of $R(S_k)$ in the full operator space.

2.3. Stationary state degeneracy in the presence of multiple non-abelian strong symmetries

We now derive the main result of this article: the lower bound on the dimension of the nullspace in the case of multiple, non-abelian strong symmetries. We achieve this via the the following theorem and proof.

Theorem 1. *Let the dynamics of a system be given by a Lindblad master equation, i.e. equation (1), with the Hamiltonian $H \in \mathcal{B}(\mathcal{H})$ and the set of Lindblad jump operators $L_l \in \mathcal{B}(\mathcal{H})$ being bounded linear operators acting over a Hilbert space $\mathcal{H}$. Let there exist a set $\{S_1, S_2, \ldots, S_n\}$ of* strong *symmetries which form a non-abelian group,*

$$[H, R(S_k)] = 0, \quad [L_l, R(S_k)] = [L_l^\dagger, R(S_k)] = 0, \quad \forall l, k, \tag{9}$$

where $R(S_k)$ is the matrix representation of the kth *strong symmetry in $\mathcal{B}(\mathcal{H})$. In general, due to these symmetries being non-abelian, we have that $[R(S_k), R(S_{k'})] \neq 0$. We then construct the group representation R via a series of irreducible representations,*

$$R = \bigoplus_{i=1}^{s} R_i, \tag{10}$$

with each representation R_i having a dimension of D_i (i.e. it is a matrix of size $D_i \times D_i$). The degeneracy (dimension) of the stationary state $\hat{\mathcal{L}}\rho_\infty = 0$ is then bounded from below by $\sum_{i=1}^{s} D_i^2$.

This theorem is applicable to both finite and infinite-size systems. However, we note that in an infinite-size system this lower bound is likely to be significantly less than the actual degeneracy due to the unbounded nature of the matrices involved.

Proof. Define $\tilde{R}_i(\cdot)$ to be an operator on the full Hilbert space acting as $R_i(\cdot)$ in the irreducible representation i and trivially in the the rest of the Hilbert space. Following the decomposition, we have $[H, \tilde{R}_i(S_k)] = [L_l, \tilde{R}_i(S_k)] = 0, \forall i, k, l,$. By Schur's representation lemma, this implies that $H, L_l, L_l^\dagger$ are multiples of the identity matrix in the R_i block [42]. This, in turn, implies that

$$[H, \{\tilde{R}_i(S_k)\}_{nm}] = [L_l, \{\tilde{R}_i(S_k)\}_{nm}] = [L_l^\dagger, \{\tilde{R}_i(S_k)\}_{nm}] = 0, \tag{11}$$

where $\{\tilde{R}_i(S_k)\}_{nm}$ indicates the matrix at position n and m within the block matrix $\tilde{R}_i(S_k)$. This means that there are $\sum_{i=1}^{s} D_i^2$ linearly independent operators that commute with $H, L_l, L_l^\dagger$. It immediately follows that these operators are in the kernel of $\hat{\mathcal{L}}^\dagger$, which has the same dimension as the kernel of $\hat{\mathcal{L}}$. □

Remark 1. Note that the individual states in the representation $|i, j\rangle$ (with $i = 1, \ldots, s$ indexing the irreducible representation and $j = 1, \ldots, D_i$ indexing the states inside the irreducible representation) can be degenerate. By Schur's lemma, both H and L_l are proportional to the identity matrix on the subspace $|i, j\rangle$. However, in general they can have further symmetry structure within the $|i, j\rangle$ subspace (e.g. they can also be multiples of the identity matrix inside these subspaces). In those cases the degeneracy will be larger than the bound; we explore an example of this situation in section 3.2.2. In many situations, however, we find there is no additional structure and that the bound is saturated.

Remark 2. Assuming standard unitary strong symmetries S_k, it is easy to see that $[L_l, S_k] = 0$ implies $[L_l^\dagger, S_k] = 0$. In this case we can dispense with the requirement $[L_l^\dagger, R(S_k)] = 0$ from equation (9) of theorem 1.

Remark 3. Due to the non-abelian nature of the symmetry group there may exist stationary states of $\hat{\mathcal{L}}\rho_{\infty,k} = 0$ that are not density matrices, i.e. $\rho_{\infty,k}^\dagger \neq \rho_{\infty,k}$. However, by nature of the dynamical map in equation (1) every initial density matrix $\rho(0)$ will always remain a valid density matrix: these unphysical states do not corrupt the lower bound we have derived as they are of trace 0 and can always be added to any physical density matrices to make another physical density matrix—provided they preserve its Hermitian nature. The D dimensional kernel always forms a basis for a convex combination of D linearly independent extreme, or fixed, points that are valid density matrices (see [43] for more details). Moreover, these states are interesting from a quantum information and computing perspective because they represent quantum coherences that can be used to store quantum information [44].

In the following, we illustrate these results with a series of examples.

3. Examples

Now that we have identified the lower bound in theorem 1, we apply this result to several physical models: a fully-connected quantum network, the Heisenberg model, and the Hubbard model.

In each example, we use exact diagonalization to compute the steady state degeneracy numerically using the QuTiP library [45, 46], and compare the numerical results with the lower bound in theorem 1.

3.1. Fully-connected quantum network

As our first example, we consider a fully-connected quantum network used as a simple model for studying the role of symmetries in energy transport in molecules [29, 47]. The model describes an exciton hopping between a series of interconnected lattice sites, pictured in figure 1. Similar lattice models are frequently used to represent the dynamics of atoms in optical lattices, electrons in quantum-dot arrays, and photons in photonic waveguides or quantum circuits [48]. These types of models have also proven useful in studying excitonic transport in photosynthetic light harvesting systems [49, 50].

The Hilbert space is spanned by the basis $\{|0\rangle, |1\rangle, |2\rangle, \ldots, |N\rangle\}$ where $|i\rangle$ denotes the state with an exciton on site $i = 1, \ldots, N$ while $|0\rangle$ is the ground state characterised by the absence

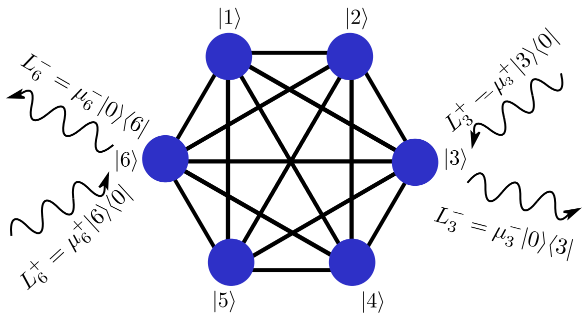

Figure 1. Sketch of the fully-connected network described in the text for the particular case of $N = 6$ sites. Solid lines represent coherent hopping between sites. The wavy arrows represent absorption and emission of excitons between the system and the environment.

of any excitation. In this basis, the Hamiltonian of the system reads

$$H = \varepsilon_g|0\rangle\langle 0| + \varepsilon\sum_{i=1}^{N}|i\rangle\langle i| + h\sum_{i\neq j}|i\rangle\langle j| = \begin{bmatrix} \varepsilon_g & 0 & 0 & \dots & 0 \\ 0 & \varepsilon & h & \dots & h \\ 0 & h & \varepsilon & \dots & h \\ \vdots & \vdots & \vdots & \ddots & \vdots \\ 0 & h & h & \dots & \varepsilon \end{bmatrix}, \tag{12}$$

where ε_g, ε and h play the role of ground state, excitation and kinetic energy scales respectively.

In order to drive a current through the network some of the lattice sites are connected to thermal baths which each interact with the system via the jump operators

$$\begin{aligned} L_j^+ &= \mu_j^+|j\rangle\langle 0|, \\ L_j^- &= \mu_j^-|0\rangle\langle j|. \end{aligned} \tag{13}$$

These operators describe the absorption and emission of an exciton on site j where $\mu_j^\pm$ is the relevant probability of that process.

The Liouvillian is invariant under the permutation of any two sites which are not connected to the thermal baths. This symmetry can be described by the exchange operator for sites i and j

$$P_{ij} = I - |i\rangle\langle i| - |j\rangle\langle j| + |i\rangle\langle j| + |j\rangle\langle i|. \tag{14}$$

The exchange operators that do not act on the bath sites (we label the bath sites as $a, b, \dots.$) then form a series of strong symmetries:

$$[H, P_{ij}] = 0, \quad [L_a^\pm, P_{ij}] = [L_b^\pm, P_{ij}] = \dots = 0, \quad \forall i, j \neq a, b, \dots. \tag{15}$$

Moreover, these operators do not necessarily commute $[P_{i,j}, P_{k,l}] \neq 0\, \forall i, j, k, l$ and thus constitute a set of non-abelian strong symmetries in this open quantum system.

More generally, we can say that every element A formed from different products of exchange elements, and belonging to the permutation group P,

$$A = \prod_{i,j} P_{ij}, \tag{16}$$

Table 1. Steady state degeneracy of the dissipative quantum network pictured in figure 1 for various system sizes, N. Two sites are always coupled to the baths. Predicted degeneracy is calculated using theorem 1 while the actual degeneracy is calculated by exact diagonalization of the matrix representation of the Liouvillian superoperator.

N	Degeneracy lower bound	Actual degeneracy
3	1	1
5	5	5
10	50	50
20	290	290
50	2210	2210

is a strong symmetry, i.e.,

$$[H, A] = 0, \quad [L_l, A] = 0, \quad \forall l. \tag{17}$$

It then follows that these group elements are thus left null eigenvectors of the Liouvillian [20, 21]

$$\mathcal{L}^{\dagger}(A) = 0. \tag{18}$$

Now suppose we label the sites which are uncoupled form the baths as $1, 2, \ldots, n$. An arbitrary permutation operator can then be block diagonalized as follows

$$A = \begin{bmatrix} R_n(A) & 0 \\ 0 & I_{N-n} \end{bmatrix}, \tag{19}$$

where $R_n(A)$ is the natural representation of A, and acts on the space spanned by $|1\rangle$, $|2\rangle$, $\ldots$, $|n\rangle$. Meanwhile, I_{N-n} acts on the remaining space, spanned by $|0\rangle$, $|n+1\rangle$, $|n+2\rangle$, $\ldots$, $|N\rangle$. This block-diagonal structure should emerge in the stationary states of the model. Moreover, the natural representation is reducible as it can be written as the direct sum of the irreducible, trivial and standard representations [51]

$$R_n(A) = R_{\mathrm{t}}(A) \oplus R_{\mathrm{s}}(A), \tag{20}$$

whose ranks are 1 and $n-1$, respectively. Hence, the permutation operator P is further block diagonalized

$$A = \begin{bmatrix} 1 & 0 & 0 \\ 0 & R_{\mathrm{s}}(P) & 0 \\ 0 & 0 & I_{N-n} \end{bmatrix}. \tag{21}$$

We have thus found an irreducible representation of the strong symmetries and since the left kernel of $\mathcal{L}$ contains all possible A, by theorem 1, its dimension must be at least $(n-1)^2 + 1$. Furthermore, for every left null vector of $\mathcal{L}$, there is a corresponding right null vector and the dimension of the right kernel is equal to the left kernel dimension. Thus the stationary state degeneracy of this model is at least $(n-1)^2 + 1$.

In table 1 we compare this result to those obtained via exact diagonalization of the full Liouvillian. The results are in complete agreement for all the system sizes we are able to reach and the bound is always completely saturated.

Additionally, we can explicitly show how the decomposition in equation (20) is reflected in the long-time states of the system. The non-trivial part of A acts on the space spanned by $\{|1\rangle$,

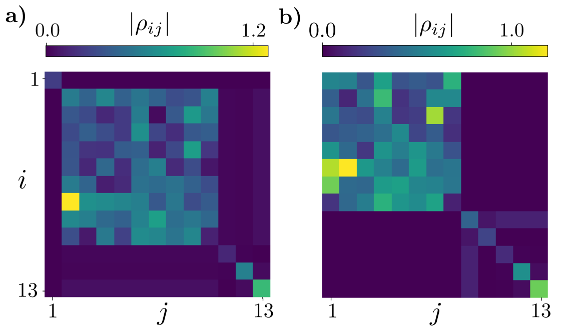

Figure 2. Plots of the matrix structure of the stationary states, with i and j indexing the matrix elements. (a, b) Example stationary state of an $N = 12$ site system. Parameters are: $\varepsilon_g = 0$, $\varepsilon = 10$ and $h = 20$. Three sites are coupled to thermal baths with coupling strengths $\mu_{10}^- = 0.6$, $\mu_{10}^+ = 0.3$, $\mu_{11}^- = 0.2$, $\mu_{11}^+ = 0.5$, $\mu_{12}^- = 0.2$, and $\mu_{12}^+ = 0.8$. (a) Absolute magnitude of the matrix elements of one of the stationary states in the configuration basis where i and j run over the basis states $\{|0\rangle, |1\rangle, \ldots, |12\rangle\}$. (b) Absolute magnitude of the matrix elements of the same stationary state but in the basis corresponding to representations of permutation group where i and j run over the basis states $\{|\psi_1\rangle, |\psi_2\rangle, \ldots, |\psi_n\rangle, |\phi_t\rangle, |0\rangle, |10\rangle, |11\rangle, |12\rangle\}$.

$|2\rangle, \ldots, |n\rangle\}$ and to explicitly uncover the decomposition in equation (20) we change from this configuration basis to a new one:

$$\{|1\rangle, |2\rangle, \ldots, |n\rangle\} \rightarrow \{|\phi_t\rangle, |\psi_1\rangle, \ldots, |\psi_{n-1}\rangle\}, \tag{22}$$

where $|\phi_t\rangle$ is the trivial representation and is defined as

$$|\phi_t\rangle = \frac{1}{\sqrt{n}} \sum_{i=1}^{n} |i\rangle, \tag{23}$$

which satisfies $R_n(A)|\phi_t\rangle = |\phi_t\rangle$. Meanwhile the $|\psi_i\rangle$ form the standard representation $R_s(P)$ and describe $n-1$ linearly independent basis vectors whose coefficients in this same basis sum to 0 and thus $\langle\phi_t|\psi_i\rangle = 0 \forall i$. Note that the exciton is fully delocalised over the sites uncoupled from the baths in all states in this new basis.

In figure 2 we provide example plots of the stationary states of the system following exact diagonalization. The block-diagonal structure of the steady states in the two bases exposes the decompositions in equations (20) and (21), which provide a natural structure to the steady states of the system.

Finally, we note that the Hamiltonian and every Lindblad operators can be likewise block-diagonalized within this decomposition, and take the form:

$$H = \begin{bmatrix} \varepsilon + (n-1)h & 0 & h^\dagger \\ 0 & (\varepsilon - h)I_{n-1} & 0 \\ h & 0 & H_o \end{bmatrix}, \quad L_i^\pm = \begin{bmatrix} 0 & 0 & 0 \\ 0 & 0 & 0 \\ 0 & 0 & L_{i,o}^\pm \end{bmatrix}. \tag{24}$$

Here, we have set, without loss of generality, the ground state energy ε_g to zero.

3.2. XXX Heisenberg model

For our second example we turn our attention to a many-body system with continuous non-abelian symmetries: the quantum Heisenberg model with zero magnetic field. Most of the

Table 2. Decomposition of the SU(2) symmetry of the *N*-site XXX Heisenberg model into a series of fundamental, irreducible representations. For example, $\mathbf{2}^{\otimes 2} = \mathbf{3} \oplus \mathbf{1}$ refers to the decomposition of two spin 1/2s into a spin singlet and triplet. The third column is the corresponding lower bound for the stationary state degeneracy of the open XXX model, provided the dissipation preserves the overall SU(2) symmetry.

N	Decomposition of representation	Degeneracy lower bound
2	$\mathbf{2}^{\otimes 2} = \mathbf{3} \oplus \mathbf{1}$	$3^2 + 1^2 = 10$
3	$\mathbf{2}^{\otimes 3} = \mathbf{4} \oplus (2 \times \mathbf{2})$	$4^2 + 2^2 = 20$
4	$\mathbf{2}^{\otimes 4} = \mathbf{5} \oplus (3 \times \mathbf{3}) \oplus (2 \times \mathbf{1})$	$5^2 + 3^2 + 1^2 = 35$
5	$\mathbf{2}^{\otimes 5} = \mathbf{6} \oplus (4 \times \mathbf{4}) \oplus (5 \times \mathbf{2})$	$6^2 + 4^2 + 2^2 = 56$
6	$\mathbf{2}^{\otimes 6} = \mathbf{7} \oplus (5 \times \mathbf{5}) \oplus (9 \times \mathbf{3}) \oplus (5 \times \mathbf{1})$	$7^2 + 5^2 + 3^2 + 1^2 = 84$
7	$\mathbf{2}^{\otimes 7} = \mathbf{8} \oplus (6 \times \mathbf{6}) \oplus (14 \times \mathbf{4}) \oplus (14 \times \mathbf{2})$	$8^2 + 6^2 + 4^2 + 2^2 = 120$

following discussion, however, will be valid for general SU(2) symmetric Hamiltonians. We consider the open isotropic XXX spin chain with the Hamiltonian

$$H = \sum_{i=1}^{N-1} (\sigma_i^x \sigma_{i+1}^x + \sigma_i^y \sigma_{i+1}^y + \sigma_i^z \sigma_{i+1}^z), \tag{25}$$

where $\sigma_i^{x,y,z}$ denotes the x, y, z Pauli operator on site i. Importantly, we assume the dissipation in the system commutes with each of the the total spin operators $S^{x,y,z} = \sum_{i=1}^{N} \sigma_i^{x,y,z}$. If this is the case then the system has an SU(2) symmetry as the total spin operators each form a strong symmetry

$$[H, S^x] = [H, S^y] = [H, S^z] = 0, \tag{26}$$

and are non-abelian as we have $[S^\alpha, S^\beta] \neq 0, \alpha \neq \beta$.

In order to apply our theorem we need to decompose these symmetries over the *N*-sites into a series of irreducible representations. We use **2** to denote the fundamental representation of the SU(2) symmetry on a single site, where, more generally, **n** denotes a representation of this Lie algebra over an n dimensional space [52]. We use this notation to perform the required decomposition and as a result the lower bound of stationary state degeneracy can be determined using theorem 1. In table 2 we depict this, showing the decomposition of the spin SU(2) symmetry over an *N*-site system and the corresponding lower bound on the stationary state degeneracy, which grows as $O(N^3)$

In order to demonstrate the strength of this bound, we consider coupling explicitly the system to two different SU(2) preserving environments.

3.2.1. Random coupling dissipation. In the first case we couple the system to an environment which induces dissipation between arbitrary pairs of sites with random (complex) strength. Such a model should be interesting for understanding effects of dissipative disorder on thermalization and transport properties in a quantum many-body system. The master equatio takes the form

$$\begin{aligned} \dot{\rho} &= -i[H, \rho] + \sum_l (2L_l^\dagger \rho L_l - \{L_l^\dagger L_l \rho\}), \\ L_l &= \sum_{i,j} M_l^{ij} (\sigma_i^x \sigma_j^x + \sigma_i^y \sigma_j^y + \sigma_i^z \sigma_j^z), \end{aligned} \tag{27}$$

where each M_l is an arbitrary complex matrix with i, j indexing its elements. The jump operators L_l describe dissipation proportional to the dipole interaction between sites i and j, with M_l^{ij}

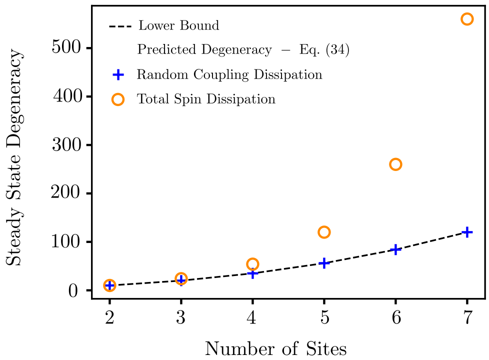

Figure 3. Plot of stationary state degeneracy vs system size for the open XXX Heisenberg model with dissipation which preserves the SU(2) symmetry structure. Two different types of dissipation are considered, 'total spin dissipation' and 'arbitrary coupling dissipation' described in equations (27) and (28), respectively. Data points are calculated by exact diagonalization of the Liouvillian of the system. The dashed black line is the theoretical lower bound calculated using theorem 1 (see table 2), while the dashed line is the prediction from equation (34) which accounts for the additional structure of the nullspace of the system in the case of total spin dissipation.

quantifying the strength of this interaction. While not fully realistic, this type of dissipation is instructive to our theory. The Lindblad operator commutes with all generators of the SU(2) symmetry and thus the total spin operators form a series of non-abelian strong symmetries.

We test our lower bound by computing the stationary state degeneracy numerically via exact diagonalization. We generate the M_l^{ij} by drawing the real and imaginary parts as random numbers with a uniform distribution over the interval $[-1, 1]$. We then average the stationary state degeneracy over a series of instances of this dissipation. As shown in figure 3, we find that our bound is saturated and provides an exact description of the stationary state degeneracy of the system.

3.2.2. Total spin dissipation. As a second example of dissipation which preserves the SU(2) symmetry, we consider dissipation induced by the Casimir operator

$$L = S^2 = (S^x)^2 + (S^y)^2 + (S^z)^2, \tag{28}$$

such that the master equation reads

$$\dot{\rho} = -\mathrm{i}[H, \rho] + \gamma(2L\rho L^\dagger - \{L^\dagger L, \rho\}). \tag{29}$$

Since $[S^2, S^x] = [S^2, S^y] = [S^2, S^z] = 0$, the SU(2) symmetry is not broken by the dissipation and thus, again, we have a set of non-abelian strong symmetries.

We compute the actual stationary state degeneracy of this Liouvillian numerically and compare to our theory in table 2. We report the results in figure 3. They indicate that for systems with site number $N > 2$, the actual number of stationary states is much greater than the lower bound. We can, however, explain this difference within the structure of our theory. There is a further structure to the states within each irreducible representation (see remark 1 in theorem 1) which, consequently, increases the steady state degeneracy above the lower bound.

Since $L = S^2$ commutes with the Hamiltonian and L is Hermitian there is a basis in which both H and L are mutually diagonal. Clearly, $\hat{\mathcal{L}}$ is also diagonal in this basis. We can write the

Casimir operator as,

$$L = \sum_{i=1}^{s} \sum_{j=1}^{D_i} \sum_{x=1}^{M_i} c_i |i, j, x\rangle\langle i, j, x|, \tag{30}$$

where j labels states within each irreducible representation and x labels the M_i further states in the $|i, j\rangle$ subspace, which have well-defined total angular momentum and angular momentum in the z direction. For example, $M_1 = 1, M_2 = 4$ and $M_3 = 5$ for the 5-site system whose decomposition is shown in table 2. We note that L is the identity within each $|i, j\rangle$ subspace.

By Schur's lemma H is proportional to the identity matrix in each subspace i,

$$H = \sum_{i=1}^{s} \sum_{j=1}^{D_i} \sum_{x=1}^{M_i} \sum_{y=1}^{M_i} h_i(x, y)|i, j, x\rangle\langle i, j, y|. \tag{31}$$

We can then diagonalize H in the $|i, j\rangle$ subspace,

$$H = \sum_{i=1}^{s} \sum_{j=1}^{D_i} \sum_{x=1}^{M_i} E_x^{(i)} |i, j, x\rangle\langle i, j, x|, \tag{32}$$

where $E_x^{(i)}$ are the energies within the irreducible representation i. Note that there may be further accidental degeneracies in the energies, or more generally additional symmetry structure guaranteeing that for some energies $E_x^{(i)} = E_{x'}^{(i)}$.

It is clear that $|i, j, x\rangle$ is an eigenstate of both H and L with the same respective eigenvalues $\forall j$ and every pair x, x' that has the same energy $E_x^{(i)} = E_{x'}^{(i)}$. Therefore,

$$\hat{\mathcal{L}}|i, j, x\rangle\langle i, j', x'| = 0, \quad \forall x, x'|E_x^{(i)} = E_{x'}^{(i)}. \tag{33}$$

Hence, assuming that the energies $E_x^{(i)}$ are all distinct the stationary state degeneracy is

$$N_\mathrm{s} = \sum_{i=1}^{s} M_i \times D_i^2, \tag{34}$$

which is larger than the lower bound of theorem 1. We find that this new prediction for the degeneracy, which accounts for the additional symmetry structure, matches the exact-diagonalization results, see figure 3.

3.3. Hubbard model

As a final example we consider the Hubbard model under local dissipation. The Hubbard model is a simple but very successful physical model of solid state systems under the tight-binding approximation. For sake of simplicity we focus on the one-dimensional case. The Hamiltonian for an N-site chain reads

$$H = -t \sum_{\langle ij\rangle,\sigma} \left(c_{i,\sigma}^{\dagger} c_{j,\sigma} + H.c. \right) + U \sum_{i=1}^{N} n_{i,\uparrow} n_{i,\downarrow}, \tag{35}$$

where $c_{i,\sigma}$ and its adjoint are the annihilation and creation operators for a fermion of spin $\sigma \in \{\uparrow, \downarrow\}$ on site i. In addition, $n_{i,\sigma}$ is the number operator for a spin σ on site i. The quantities t and U are, respectively, kinetic and interaction energy scales, with the summation in the kinetic term taken over nearest-neighbour pairs $\langle ij\rangle$ on the lattice.

The Hubbard model has a rich symmetry structure which has made it a natural environment for inducing exotic non-equilibrium phases through dissipation [53, 54]. The continuous symmetry of this model is SO(4) and because $\mathrm{SO}(4) = \mathrm{SU}(2) \times \mathrm{SU}(2)/Z_2$ there are two commuting SU(2) symmetries within the model [55].

The first of these is the spin symmetry, generated by the spin operators

$$S^{+} = \sum_{j=1}^{N} c^{\dagger}_{j,\uparrow} c_{j,\downarrow}, \quad S^{-} = \sum_{j=1}^{N} c^{\dagger}_{j,\downarrow} c_{j,\uparrow}, \quad S^{z} = \frac{1}{2}\sum_{j=1}^{N} (n_{j,\uparrow} - n_{j,\downarrow}), \tag{36}$$

which satisfy the SU(2) relations

$$[S^z, S^{\pm}] = \pm S^{\pm}, \quad [S^+, S^-] = 2S^z, \quad [H, S^z] = [H, S^{\pm}] = 0. \tag{37}$$

The second, hidden, symmetry is often referred to as the 'η-symmetry', and relates to spinless quasi-particles (doublons and holons). It plays an important role in the formation of superconducting eigenstates of the Hubbard model [56]. This η-symmetry is generated by the operators

$$\eta^{+} = \sum_{i=1}^{N} (-1)^{i} c^{\dagger}_{i,\uparrow} c^{\dagger}_{i,\downarrow}, \quad \eta^{-} = (\eta^{+})^{\dagger}, \quad \eta^{z} = \frac{1}{2}\sum_{i=1}^{N} (n_{i,\uparrow} + n_{i,\downarrow} - 1), \tag{38}$$

which satisfy the relations

$$[\eta^z, \eta^{\pm}] = \pm \eta^{\pm}, \quad [\eta^+, \eta^-] = 2\eta^z, \quad [H, \eta^z] = [H, \eta^{\pm}] = 0. \tag{39}$$

The two SU(2) symmetries are abelian

$$[S^{\alpha}, \eta^{\beta}] = 0, \quad \alpha, \beta = +, -, z \tag{40}$$

but clearly the operators which form each SU(2) symmetry are not.

To study the representation of this $\mathrm{SU}(2) \times \mathrm{SU}(2)$ symmetry over an N-site lattice, we first need to describe its representation in terms of a single site. Since the two SU(2) symmetries are commuting, we are able to describe their representation with two individual representations. We define a representation of $\mathrm{SU}(2) \times \mathrm{SU}(2)$ as $(\mathbf{m}, \mathbf{n})$ where $\mathbf{m}$ and $\mathbf{n}$ describe the representations of the first and second SU(2) symmetries respectively. For instance, we can decompose the single-site $\mathrm{SU}(2) \times \mathrm{SU}(2)$ group as

$$(\mathbf{2}, \mathbf{1} \oplus \mathbf{1}) \oplus (\mathbf{1} \oplus \mathbf{1}, \mathbf{2}). \tag{41}$$

This means that the four-dimensional single-site Hilbert space is a direct sum of two invariant subspaces. In the first subspace the representation of the spin symmetry is two dimensional and the representation of η symmetry is the direct sum of two trivial representations, while in the second subspace the converse is true. This can be seen by writing down the spin and η operators on the one-site Hilbert space in explicit matrix form

$$S^x = \frac{1}{2}\begin{bmatrix} 0 & 0 & 0 & 0 \\ 0 & 0 & 0 & 0 \\ 0 & 0 & 0 & 1 \\ 0 & 0 & 1 & 0 \end{bmatrix}, \quad S^z = \frac{1}{2}\begin{bmatrix} 0 & 0 & 0 & 0 \\ 0 & 0 & 0 & 0 \\ 0 & 0 & -1 & 0 \\ 0 & 0 & 0 & 1 \end{bmatrix}, \tag{42}$$

$$\eta^x = \frac{1}{2}\begin{bmatrix} 0 & 1 & 0 & 0 \\ 1 & 0 & 0 & 0 \\ 0 & 0 & 0 & 0 \\ 0 & 0 & 0 & 0 \end{bmatrix}, \quad \eta^z = \frac{1}{2}\begin{bmatrix} -1 & 0 & 0 & 0 \\ 0 & 1 & 0 & 0 \\ 0 & 0 & 0 & 0 \\ 0 & 0 & 0 & 0 \end{bmatrix}. \tag{43}$$

Table 3. The symmetric reduction and corresponding lower bound of the stationary state degeneracy for the spin-dephased Fermi–Hubbard model, which is SU(2) × U(1) symmetric. The second column lists the unique fundamental representations of this SU(2) × U(1) symmetry over an *N*-site lattice. The third column is the lower bound on the null space dimension, calculated using theorem 1. The fourth column is the actual stationary state degeneracy obtained from numerically diagonalizing the Liouvillian of the system.

N	Irreducible representations	Degeneracy lower bound	Actual degeneracy
2	$\mathbf{3}_0$ $\mathbf{2}_1\mathbf{2}_{-1}$ $\mathbf{1}_2\mathbf{1}_0\mathbf{1}_{-2}$	20	20
3	$\mathbf{4}_0$ $\mathbf{3}_1\mathbf{3}_{-1}$ $\mathbf{2}_2\mathbf{2}_0\mathbf{2}_{-2}$ $\mathbf{1}_3\mathbf{1}_1\mathbf{1}_{-1}\mathbf{1}_{-3}$	50	50
4	$\mathbf{5}_0$ $\mathbf{4}_1\mathbf{4}_{-1}$ $\mathbf{3}_2\mathbf{3}_0\mathbf{3}_{-2}$ $\mathbf{2}_3\mathbf{2}_1\mathbf{2}_{-1}\mathbf{2}_{-3}$ $\mathbf{1}_4\mathbf{1}_2\mathbf{1}_0\mathbf{1}_{-2}\mathbf{1}_{-4}$	105	105
5	$\mathbf{6}_0$ $\mathbf{5}_1\mathbf{5}_{-1}$ $\mathbf{4}_2\mathbf{4}_0\mathbf{4}_{-2}$ $\mathbf{3}_3\mathbf{3}_1\mathbf{3}_{-1}\mathbf{3}_{-3}$ $\mathbf{2}_4\mathbf{2}_2\mathbf{2}_0\mathbf{2}_{-4}\mathbf{2}_{-2}$ $\mathbf{1}_5\mathbf{1}_3\mathbf{1}_1$ $\mathbf{1}_{-1}\mathbf{1}_{-3}\mathbf{1}_{-5}$	196	196

The basis of the above matrices is $\{|\text{vac}\rangle, |\uparrow\downarrow\rangle, |\downarrow\rangle, |\uparrow\rangle\}$, where the arrows indicate the presence of a fermion of either spin 'up' or 'down'.

We now couple the Hubbard Hamitonian in equation (35) to an environment which induces homogeneous, local spin-dephasing. The dynamics is modelled, under the Markov approximation, via the Lindblad master equation

$$\dot{\rho} = -\mathrm{i}[H, \rho] + \gamma \sum_{l=1}^{N} (2L_l \rho L_l^\dagger - \{L_l^\dagger L_l \rho\}),$$

with the Lindblad operators

$$L_l = s_l^z = \frac{1}{2}(n_{l,\uparrow} - n_{l,\downarrow}). \tag{44}$$

A possible experimental implementation for this master equation is discussed in reference [54] where the spin dephasing was shown to induce superconducting order in the long-time limit of the system. Under this dephasing, the η symmetry is preserved $[L_l, \eta^{+,-,z}] = 0$ while the spin SU(2) symmetry is broken into a U(1) symmetry since $[L_l, S^{\pm}] \neq 0$ and $[L_l, S^z] = 0$.

We represent this SU(2) × U(1) symmetry over the one-site space as

$$\mathbf{2}_0 \oplus \mathbf{1}_1 \oplus \mathbf{1}_{-1}, \tag{45}$$

where the bold numbers denote the representation of the remaining SU(2) symmetry, and the subscript indexes the value of S^z (the U(1) symmetry) in that representation. With this notation, we can then construct the representation over the full Hilbert space for N sites. For example, the representation of the 2-site system is

$$(\mathbf{2}_0 \oplus \mathbf{1}_1 \oplus \mathbf{1}_{-1}) \otimes (\mathbf{2}_0 \oplus \mathbf{1}_1 \oplus \mathbf{1}_{-1}) \\ = \mathbf{3}_0 \oplus \mathbf{1}_0 \oplus \mathbf{2}_1 \oplus \mathbf{2}_{-1} \oplus \mathbf{2}_1 \oplus \mathbf{1}_2 \oplus \mathbf{1}_0 \oplus \mathbf{2}_{-1} \oplus \mathbf{1}_0 \oplus \mathbf{1}_{-2}, \tag{46}$$

which can immediately be extended to N sites. Using this representation we can apply theorem 1 and predict the lower bound of the stationary space dimension. We find that the lower bound of the null space dimension for an N site system is

$$N_s = \sum_{n=1}^{N+1} (N + 2 - n)n^2. \tag{47}$$

In table 3, we compare this lower bound with numerical exact-diagonalization results. We find that the bound is exactly saturated for the small systems where calculations are accessible; larger systems are outside numerical tractability. We notice that, for this example, the growth of this bound is $O(N^4)$, which is faster than the usual $O(N^3)$ growth because of the additional U(1) symmetry.

4. Conclusion

We have provided a lower bound on the stationary-state degeneracy of open quantum systems with multiple non-abelian symmetries. This bound is based on the decomposition of the symmetry group into a series of irreducible representations. As examples we have studied an open quantum network, the dephased XXX spin chain and a spin-dephased Hubbard model. By comparing with exact-diagonalization calculations, we have shown that the bound is saturated in most of the examples we looked at, providing crucial evidence of the strength of our bound for open quantum many-body systems. Thus we expect that if additional degeneracies are discovered in the stationary state through e.g. numerical calculations, these may hint at possible hidden symmetries in the model waiting to be discovered. Alternatively, the system may have accidental degeneracies.

Our general results here open many interesting venues for future study. The most pressing is extending the results to non-abelian dynamical symmetries. Dynamical symmetries in both closed [57], and open quantum many-body systems [40, 53, 58] have been shown to guarantee absence of any relaxation to stationarity, instead leading to persistent oscillations and complex dynamics. Our work should also be extended beyond the Markovian approximation, to include more widely applicable Redfield master equations [18]. In cases where the open system has only approximate non-abelian strong symmetries, one may expect metastable stationary states [59, 60].

This work also opens up the possibility of applying our symmetry reduction method to the study of dissipative magnetic systems [61], and other two-dimensional systems [6, 7], where the high level of symmetry reduction could be beneficial due to a lack of viable computational methods. We also anticipate further work applying our theory to dissipation-induced frustration of open quantum systems [62] due to the high entropy content of the stationary state.

Lastly, our work on the fully-connected quantum network provides a systematic method to study more complex networks with hierarchical structure and topology [47], as well as other molecular structures with a high degree of symmetry [29, 63].

Acknowledgments

We would like to thank R A Molina for useful discussions. This work has been supported by UK EPSRC Grants Nos. EP/P01058X/1, EP/P009565/1, EP/K038311/1, EPSRC National Quantum Technology Hub in Networked Quantum Information Technology (EP/M013243/1), and the European Research Council under the European Union's Seventh Framework Programme (FP7/2007-2013)/ERC Grant Agreement No. 319286 (Q-MAC). Zh Z acknowledges support from the Tsinghua University Education Foundation (TUEF).

ORCID iDs

J Tindall https://orcid.org/0000-0003-1335-8637
B Buča https://orcid.org/0000-0003-3119-412X

References

[1] D'Alessio L, Kafri Y, Polkovnikov A and Rigol M 2016 From quantum chaos and eigenstate thermalization to statistical mechanics and thermodynamics *Adv. Phys.* **65** 239–362
[2] Vidmar L and Rigol M 2016 2016 Generalized Gibbs ensemble in integrable lattice models *J. Stat. Mech.* 064007
[3] Cassidy A C, Clark C W and Rigol M 2011 Generalized thermalization in an integrable lattice system *Phys. Rev. Lett.* **106** 140405
[4] Ilievski E, Medenjak M, Prosen T and Zadnik L 2016 Quasilocal charges in integrable lattice systems *J. Stat. Mech.* 064008
[5] Benjamin D 2017 Thermalization and pseudolocality in extended quantum systems *Commun. Math. Phys.* **351** 155–200
[6] Mur-Petit J and Molina R A 2014 Chiral bound states in the continuum *Phys. Rev.* B **90** 035434
[7] Mur-Petit J and Molina R A 2020 Van Hove bound states in the continuum: localised subradiant states in finite open lattices (arXiv:2002.05959)
[8] Essler F H L, Mussardo G and Panfil M 2015 Generalized Gibbs ensembles for quantum field theories *Phys. Rev.* A **91** 051602
[9] Pozsgay B 2013 The generalized Gibbs ensemble for heisenberg spin chains *J. Stat. Mech.* P07003
[10] Ilievski E, De Nardis J, Wouters B, Caux J-S, Essler F H L and Prosen T 2015 Complete generalized Gibbs ensembles in an interacting theory *Phys. Rev. Lett.* **115** 157201
[11] Eisert J, Friesdorf M and Gogolin C 2015 Quantum many-body systems out of equilibrium *Nat. Phys.* **11** 124
[12] Calabrese P, Essler F H L and Mussardo G 2016 Introduction to quantum integrability in out of equilibrium systems *J. Stat. Mech.* 064001
[13] Wouters B, De Nardis J, Brockmann M, Fioretto D, Rigol M and Caux J-S 2014 Quenching the anisotropic Heisenberg chain: exact solution and generalized Gibbs ensemble predictions *Phys. Rev. Lett.* **113** 117202
[14] Pozsgay B, Mestyán M, Werner M A, Kormos M, Zaránd G and Takács G 2014 Correlations after quantum quenches in the *xxz* spin chain: failure of the generalized Gibbs ensemble *Phys. Rev. Lett.* **113** 117203
[15] Sotiriadis S and Martelloni G 2016 Equilibration and GGE in interacting-to-free quantum quenches in dimensions $d > 1$ *J. Phys. A: Math. Theor.* **49** 095002
[16] Lindblad G 1976 On the generators of quantum dynamical semigroups *Commun. Math. Phys.* **48** 119–30
[17] Gorini V, Kossakowski A and Sudarshan E C G 1976 Completely positive dynamical semigroups of n-level systems *J. Math. Phys.* **17** 821–5
[18] Breuer H P and Petruccione F 2007 *The Theory of Open Quantum Systems* (Oxford: Oxford University Press)
[19] Baumgartner B and Narnhofer H 2008 Analysis of quantum semigroups with GKS–Lindblad generators: II. General *J. Phys. A: Math. Theor.* **41** 395303

[20] Buča B and Prosen T 2012 A note on symmetry reductions of the Lindblad equation: transport in constrained open spin chains *New J. Phys.* **14** 073007
[21] Albert V V and Jiang L 2014 Symmetries and conserved quantities in lindblad master equations *Phys. Rev.* A **89** 022118
[22] Albert V V, Barry B, Fraas M and Jiang L 2016 Geometry and response of lindbladians *Phys. Rev.* X **6** 041031
[23] Mirrahimi M, Leghtas Z, Albert V V, Touzard S, Schoelkopf R J, Jiang L and Devoret M H 2014 Dynamically protected cat-qubits: a new paradigm for universal quantum computation *New J. Phys.* **16** 045014
[24] Garbe L, Bina M, Keller A, Paris M G A and Felicetti S 2019 Critical quantum metrology with a finite-component quantum phase transition (arXiv:1910.00604)
[25] Liu J, Segal D and Hanna G 2019 Loss-free excitonic quantum battery *J. Phys. Chem.* C **123** 18303–14
[26] Manzano D and Hurtado P I 2014 Symmetry and the thermodynamics of currents in open quantum systems *Phys. Rev.* B **90** 125138
[27] Manzano D, Chuang C and Cao J 2016 Quantum transport in d-dimensional lattices *New J. Phys.* **18** 043044
[28] Ilievski E and Prosen T 2014 Exact steady state manifold of a boundary driven spin-1 Lai–Sutherland chain *Nucl. Phys.* B **882** 485–500
[29] Thingna J, Manzano D and Cao J 2016 Dynamical signatures of molecular symmetries in nonequilibrium quantum transport *Sci. Rep.* **6** 28027
[30] Žnidarič M 2016 Dissipative remote-state preparation in an interacting medium *Phys. Rev. Lett.* **116** 030403
[31] Kouzelis A, Macieszczak K, Minář J and Lesanovsky I 2019 Dissipative quantum state preparation and metastability in two-photon micromasers (arXiv:1906.03933)
[32] Pavel Kos and Prosen T 2017 Time-dependent correlation functions in open quadratic fermionic systems *J. Stat. Mech.* 123103
[33] van Caspel M and Gritsev V 2018 Symmetry-protected coherent relaxation of open quantum systems *Phys. Rev.* A **97** 052106
[34] Wolff S, Sheikhan A and Kollath C 2016 Dissipative time evolution of a chiral state after a quantum quench *Phys. Rev.* A **94** 043609
[35] Jaschke D, Carr L D and de Vega I 2019 Thermalization in the quantum Ising model–approximations, limits, and beyond *Quantum Science and Technology* **4** 034002
[36] Lazarides A, Roy S, Piazza F and Moessner R 2019 On time crystallinity in dissipative floquet systems (arXiv:1904.04820)
[37] Gambetta F M, Carollo F, Marcuzzi M, Garrahan J P and Lesanovsky I 2019 Discrete time crystals in the absence of manifest symmetries or disorder in open quantum systems *Phys. Rev. Lett.* **122** 015701
[38] Riera-Campeny A, Moreno-Cardoner M and Sanpera A 2019 Time crystallinity in open quantum systems (arXiv:1908.11339)
[39] Thingna J, Manzano D and Cao J 2019 Magnetic field induced symmetry breaking in nonequilibrium quantum networks (arXiv:1909.09549)
[40] Tindall J, Muñoz C S, Buča B and Jaksch D 2020 Quantum synchronisation enabled by dynamical symmetries and dissipation *New J. Phys.* **22** 013026
[41] Gardiner C W and Zoller P 2000 *Quantum Noise* 2nd edn (Berlin: Springer)
[42] Cornwell J F 1997 *Group Theory in Physics* (Amsterdam: Elsevier)
[43] Wolf M M 2012 Quantum channels and operations: guided tour lecture notes available at: http://-m5.ma.tum.de/foswiki/pub/M5/Allgemeines/MichaelWolf/QChannelLecture.pdf
[44] Victor V A 2017 Lindbladians with multiple steady states: theory and applications *PhD Thesis* Yale University (arXiv:1802.00010)
[45] Johansson J R, Nation P D and QuTiP F N 2012 An open-source Python framework for the dynamics of open quantum systems *Comput. Phys. Commun.* **183** 1760–72
[46] Johansson J R, Nation P D and Franco N 2013 QuTiP 2: a Python framework for the dynamics of open quantum systems *Comput. Phys. Commun.* **184** 1234–40
[47] Manzano D and Hurtado P I 2018 Harnessing symmetry to control quantum transport *Adv. Phys.* **67** 1–67
[48] Fernández-Hurtado V, Mur-Petit J, García-Ripoll J J and Molina R A 2014 Lattice scars: surviving in an open discrete billiard *New J. Phys.* **16** 035005

[49] Cao J and Silbey R J 2009 Optimization of exciton trapping in energy transfer processes *J. Phys. Chem.* A **113** 13825–38
[50] Walschaers M, Fernandez-de-Cossio Diaz J, Mulet R and Buchleitner A 2013 Optimally designed quantum transport across disordered networks *Phys. Rev. Lett.* **111** 180601
[51] Fulton W and Harris J 2004 *Representation Theory* (New York: Springer)
[52] Howard G 2018 *Lie Algebras in Particle Physics* (Boca Raton, FL: CRC Press)
[53] Buca B, Joseph T and Jaksch D 2019 Non-stationary coherent quantum many-body dynamics through dissipation *Nat. Commun.* **10** 1730
[54] Joseph T, Buca B, Coulthard J and Jaksch D Jul 2019 Heating-induced long-range η pairing in the Hubbard model *Phys. Rev. Lett.* **123** 030603
[55] Essler F H L, Frahm H, Frank G, Klümper A and Vladimir E K 2005 *The One-Dimensional Hubbard Model* (Cambridge: Cambridge University Press)
[56] Yang C N 1989 η pairing and off-diagonal long-range order in a Hubbard model *Phys. Rev. Lett.* **63** 2144–7
[57] Medenjak M, Buca B and Jaksch D 2019 The isolated Heisenberg magnet as a quantum time crystal (arXiv:1905.08266)
[58] Buča B and Jaksch D 2019 Dissipation induced nonstationarity in a quantum gas *Phys. Rev. Lett.* **123** 260401
[59] Macieszczak K, Guţă M, Lesanovsky I and Garrahan J P 2016 Towards a theory of metastability in open quantum dynamics *Phys. Rev. Lett.* **116** 240404
[60] Rose D C, Macieszczak K, Lesanovsky I and Garrahan J P 2016 Metastability in an open quantum Ising model *Phys. Rev.* E **94** 052132
[61] Manzano D, Chuang C and Cao J 2016 Quantum transport in d-dimensional lattices *New J. Phys.* **18** 043044
[62] Lacroix C, Mendels P and Mila F 2011 *Introduction to Frustrated Magnetism: Materials, Experiments, Theory* vol 164 (Berlin: Springer)
[63] Blackmore J A, Caldwell L, Gregory P D, Bridge E M, Sawant R, Aldegunde J, Mur-Petit J, Jaksch D, Jeremy M H and Sauer B E *et al* 2018 Ultracold molecules for quantum simulation: rotational coherences in CaF and RbCs *Quantum Science and Technology* **4** 014010